

RESEARCH

Open Access



TPEN attenuates amyloid- β_{25-35} -induced neuronal damage with changes in the electrophysiological properties of voltage-gated sodium and potassium channels

Wen-bo Chen¹, Yu-xiang Wang², Hong-gang Wang¹, Di An¹, Dan Sun¹, Pan Li³, Tao Zhang¹, Wan-ge Lu¹ and Yan-qiang Liu^{1*} 

Abstract

To understand the role of intracellular zinc ion (Zn^{2+}) dysregulation in mediating age-related neurodegenerative changes, particularly neurotoxicity resulting from the generation of excessive neurotoxic amyloid- β ($A\beta$) peptides, this study aimed to investigate whether N, N', N', N'-tetrakis (2-pyridylmethyl) ethylenediamine (TPEN), a Zn^{2+} -specific chelator, could attenuate $A\beta_{25-35}$ -induced neurotoxicity and the underlying electrophysiological mechanism. We used the 3-(4, 5-dimethyl-thiazol-2-yl)-2, 5-diphenyltetrazolium bromide assay to measure the viability of hippocampal neurons and performed single-cell confocal imaging to detect the concentration of Zn^{2+} in these neurons. Furthermore, we used the whole-cell patch-clamp technique to detect the evoked repetitive action potential (APs), the voltage-gated sodium and potassium (K^+) channels of primary hippocampal neurons. The analysis showed that TPEN attenuated $A\beta_{25-35}$ -induced neuronal death, reversed the $A\beta_{25-35}$ -induced increase in intracellular Zn^{2+} concentration and the frequency of APs, inhibited the increase in the maximum current density of voltage-activated sodium channel currents induced by $A\beta_{25-35}$, relieved the $A\beta_{25-35}$ -induced decrease in the peak amplitude of transient outward K^+ currents (I_A) and outward-delayed rectifier K^+ currents (I_{DR}) at different membrane potentials, and suppressed the steady-state activation and inactivation curves of I_A shifted toward the hyperpolarization direction caused by $A\beta_{25-35}$. These results suggest that $A\beta_{25-35}$ -induced neuronal damage correlated with Zn^{2+} dysregulation mediated the electrophysiological changes in the voltage-gated sodium and K^+ channels. Moreover, Zn^{2+} -specific chelator-TPEN attenuated $A\beta_{25-35}$ -induced neuronal damage by recovering the intracellular Zn^{2+} concentration.

Keywords: TPEN, $A\beta_{25-35}$, Zinc ions, Channel currents, Voltage-gated sodium channels, Voltage-gated potassium channels

Introduction

Alzheimer's disease (AD) is an age-related neurodegenerative disease characterized by progressive cognitive dysfunction and memory decline [1]. The main histopathological hallmarks of AD include extracellular senile plaques and intracellular neurofibrillary tangles [2]. Amyloid- β ($A\beta$) protein, the main component of senile

*Correspondence: liuyanq@nankai.edu.cn; liuyanq2@126.com

¹ College of Life Sciences, Nankai University, Tianjin 300071, People's Republic of China

Full list of author information is available at the end of the article



© The Author(s) 2021. **Open Access** This article is licensed under a Creative Commons Attribution 4.0 International License, which permits use, sharing, adaptation, distribution and reproduction in any medium or format, as long as you give appropriate credit to the original author(s) and the source, provide a link to the Creative Commons licence, and indicate if changes were made. The images or other third party material in this article are included in the article's Creative Commons licence, unless indicated otherwise in a credit line to the material. If material is not included in the article's Creative Commons licence and your intended use is not permitted by statutory regulation or exceeds the permitted use, you will need to obtain permission directly from the copyright holder. To view a copy of this licence, visit <http://creativecommons.org/licenses/by/4.0/>. The Creative Commons Public Domain Dedication waiver (<http://creativecommons.org/publicdomain/zero/1.0/>) applies to the data made available in this article, unless otherwise stated in a credit line to the data.

plaques, is believed to play an important role in the pathological process of AD [3]. The neurotoxic effects of A β can trigger a deleterious cascade of events, including alterations in neuronal excitability and ion permeability, oxidative stress, inflammatory processes, cell apoptosis, and loss of synapses [4–6].

Zinc ions (Zn²⁺), an essential trace element in the human body, can regulate the function of approximately 10% of human proteins [7–9]. However, Zn²⁺ is also well known for its neurotoxic effect [10]. Excess intracellular Zn²⁺ can stimulate the generation of reactive oxygen species in hippocampal neurons, causing oxidative stress and neuronal death [11]. Some evidence suggests that intracellular Zn²⁺ dysregulation may be involved in neurotoxicity caused by the generation of excessive neurotoxic A β peptides in AD and mediating age-related cognitive impairment [12, 13]. Some autopsy studies have shown an increase in Zn²⁺ concentration in amyloid plaques of AD brains [14, 15]. In the hippocampal extracellular fluid, A β released from synaptic vesicles had a high affinity for Zn²⁺ and could rapidly bind to Zn²⁺ [16]. After injection of soluble A β to the dentate granule cell layer of normal rats, the concentration of A β and free Zn²⁺ in dentate granule cells increased within 5 min, which subsequently led to the impairment of long-term potentiation and cognition [17–19]. Therefore, maintaining intracellular Zn²⁺ homeostasis may be a promising strategy for preventing AD progression. As a Zn²⁺-specific chelator, N, N, N', N'-tetrakis (2-pyridylmethyl) ethylenediamine (TPEN) has been reported to suppress the neurotoxicity induced by soluble A β , further showing a close correlation between Zn²⁺ and neurotoxicity of A β [20]. However, it is still unclear how Zn²⁺ influences A β neurotoxicity. Therefore, more experimental data are required to further clarify the role of Zn²⁺ in the neurotoxicity of A β and pathological process of AD.

In the early stages of AD, functional MRI showed neuronal hyperactivation and epileptiform discharges in the hippocampus [21, 22], further causing cognitive deficits and memory impairments [23]. In young APP/PS1 transgenic mice, the proportion of hyperactive neurons increased [24]. Acute application of soluble A β oligomers on hippocampal slices elevates intrinsic excitability in CA1 pyramidal neurons of wild-type mice [24, 25]. These results indicate that soluble A β oligomers directly induced neuronal hyperactivity and impaired cognitive function. Further evidence suggests that sodium (Na⁺) channel involvement may be related to increases in hippocampal neuron excitability caused by A β [26]. A β -induced neuronal hyperexcitation was markedly ameliorated by the presence of riluzole, a non-selective antagonist of Na⁺ channels [26]. In fact, voltage-gated Na⁺ channels (Na_v) are crucial for regulating neuronal

excitability by initiating and propagating action potentials [27, 28]. Among the nine α -subunits of Na_v, the Na_v1.1, Na_v1.2, and Na_v1.6 subtypes were mainly expressed in the mammalian central nervous system [29]. The expression of the Na_v1.6 subtype and voltage-dependent Na⁺ current density both significantly increased in Tg2576 mice (A β pathology animal model) compared with those in wild-type mice [29]. Similar results were observed in primary cultured pyramidal neurons after incubation with soluble A β [30]. Collectively, Na_v might be involved in AD development.

In neurons, voltage-gated potassium (K⁺) channels (K_v) are crucial regulators of neuronal excitability by controlling membrane repolarization and hyperpolarization [31]. Importantly, K_v is a crucial mediator of cell death and cell survival signaling pathways [31]. K_v dysfunction is involved in many diseases, such as AD. In rat hippocampal slices, the peak amplitudes of transient outward K⁺ currents (*I_A*) and outward-delayed rectifier K⁺ currents (*I_{DR}*) decreased after acute A β incubation [32]. In A β -overexpressing cultures, the excitability of neurons increased, accompanied by a decrease in *I_A* current density and K_v4 protein expression [33]. However, restoration of K_v4 protein levels by transgenes could significantly rescue A β -induced neuronal hyperactivation and memory deficits [33, 34]. In summary, K_v is closely related to AD development.

Accordingly, A β -induced neuronal deleterious cascades are involved in Zn²⁺ dysregulation and changes in the electrophysiological properties of Na_v and K_v. However, how Zn²⁺ dysregulation influences the electrophysiological properties of Na_v and K_v in A β -treated neurons remains unclear. Therefore, in this study, we first established an in vitro model of AD by exposing soluble A β _{25–35} to primary hippocampal neurons and then detected the effect of TPEN on cell viability and intracellular free Zn²⁺ concentration in A β _{25–35}-incubated hippocampal neurons. Furthermore, we evaluated the electrophysiological properties of the evoked repetitive action potential (APs), Na_v and K_v in these neurons. We aimed to understand the role of intracellular Zn²⁺ dysregulation in A β -induced neurotoxicity and hope to provide some basis for preventing and combating AD based on Zn²⁺-specific chelators.

Materials and methods

Chemicals and animals

Dulbecco's modified Eagle medium/F12 + GlutamaxTM-1, NeurobasalTM-A Medium, GlutamaxTM, fetal bovine serum, B27 supplements, antibiotics (penicillin and streptomycin), 0.25% trypsin–EDTA, and FluoZin3-AM were purchased from Gibco (Grand Island, NY, USA). Hank's balanced salt solution (HBSS) was purchased from Solarbio (Beijing,

China). DNase, cytosine β -D-arabinofuranoside (Ara-C), TPEN, poly-L-lysine, TEA-Cl, 4-AP, and tetrodotoxin were purchased from Sigma-Aldrich (MO, USA). 3-(4,5-dimethyl-thiazol-2-yl)-2, 5-diphenyltetrazolium bromide (MTT) was obtained from Amresco, Inc. (Solon, OH, USA). The chemical constructs of A β peptides were synthesized by China Peptides Co., Ltd. (Shanghai, China) using the A β _{25–35} sequence of human APP. A β _{25–35} was dissolved in ddH₂O to prepare a stock solution with a concentration of 100 mM. The concentration of A β _{25–35} used in the experiments in this study was 20 μ M. Neonatal Sprague–Dawley rats were purchased from SPF Biotechnology Co., Ltd. (Beijing, China). All experimental protocols were approved by the Ethics Committee of Nankai University.

Isolation and culture of the primary hippocampal neurons

The primary hippocampal neurons of the rats were cultured as previously described by Beaudoin, et al. [35]. Briefly, early postnatal (P0–P1) Sprague–Dawley rats (either sex) were anesthetized with 50 mg/kg sodium pentobarbital via intraperitoneal injection and then washed with 75% (vol/vol) ethanol. The rats were then decapitated, and their brains were removed and transferred into ice-cold dissociation buffer (HBSS). The hippocampi were dissected and incubated with 0.25% trypsin–EDTA (Invitrogen, UK) at 37 °C for 12 min, with gentle shaking every 5 min. After digestion, the trypsin–EDTA solution was removed, and the hippocampi were dissociated into a single-cell suspension in 10 mL Dulbecco's modified Eagle medium/F12 (Gibco, UK) medium supplemented with 10% fetal bovine serum (Gibco, UK) and 50 μ g/mL DNase (Sigma, USA) using a 1-mL pipette with a polished plastic tip. The cell suspension was centrifuged at 100 \times g for 5 min, and the cells were resuspended in the following plating medium: Dulbecco's modified Eagle medium/F12 medium supplemented with 10% fetal bovine serum, 5 unit/mL penicillin, and 50 μ g/mL streptomycin (all from Gibco, UK). The neurons were seeded into 96-well plates or 35-mm culture dishes (pre-coated with 0.1 mg/mL poly-L-lysine for 1 h and washed three times with ddH₂O before use) at a density of 120 cells/mm² in the plating medium. After 4–6 h, the plating medium was replaced with a maintenance medium, i.e., Neurobasal-A medium supplemented with 2% B27, 1% Glutamax, 50 μ g/mL streptomycin, and 5 unit/mL penicillin (all from Gibco, UK). To prevent glial overgrowth, we treated the culture with Ara-C (Sigma, USA) at a final concentration of 1–5 μ M on day 3. The neurons were cultured in a humidified 5% CO₂ incubator at 37 °C. The maintenance medium was replaced every 3 days. The cultures were grown for 8–12 days in vitro (DIV) before the experiments.

Experimental design

The cultured hippocampal neurons were divided into three groups: control group, A β _{25–35} group, and A β _{25–35} + TPEN group. Based on the results of the preliminary experiment in relation to the viability of the hippocampal neurons after the MTT assay, the optimal concentration of TPEN was 100 nM. In the A β _{25–35} group, the hippocampal neurons were treated with A β _{25–35} in the maintenance medium at a final concentration of 20 μ M for 24 h. In the A β _{25–35} + TPEN group, the hippocampal neurons were treated with TPEN in the maintenance medium at a final concentration of 100 nM for 30 min before and during exposure to A β _{25–35}.

Determination of cell viability using the MTT assay

We used the MTT assay to assess cell viability. In brief, the culture medium from the 96-well plates was removed and replaced with 90 μ L of a fresh maintenance medium after the different treatments. Ten microliters of 5 mg/mL MTT in HBSS was added to each well, and the plates were incubated at 37 °C for 4 h. The supernatant was discarded and 100 μ L DMSO solutions was added to each well. The plates were then incubated at 37 °C for 30 min. The absorbance of each sample was measured at 570 nm using a BIORAD680 plate reader (Thermo, Waltham, MA, USA). The experiments were repeated at least three times, and the results were compared to those of the control group.

Single live-cell confocal imaging

We used live-cell confocal imaging to investigate the intracellular Zn²⁺ concentration in the hippocampal neurons. Briefly, the hippocampal neurons were seeded in a 35-mm glass bottom Petri dish (Nest, China). After the corresponding treatments, the neurons were washed twice with HBSS. For intracellular Zn²⁺ imaging, the neurons were incubated in HBSS containing 2 mM FluoZin3-AM (Life Technologies, USA) and 0.02% (w/v) pluronic acid (Solarbio) at 37 °C in the dark for 1 h. They were then rinsed and maintained in HBSS. Images were captured using a laser scanning confocal microscope (TCSSP5, Leica, Germany) with a 63 \times objective.

Whole-cell patch-clamp recording from the cultured hippocampal neurons

Based on the procedures of Wang, et al. [36], the whole-cell patch-clamp technique was performed to record APs, I_{Na} and K_v currents at 22–25 °C. The recording pipettes were pulled using a multi-stage micropipette puller (P-97, Sutter Instruments, Novato, CA, USA) and a borosilicate capillary glass. The tip resistance of the pipettes was 3–5 M Ω after

being filled with the intracellular solution. The hippocampal neurons were then incubated with extracellular solution. We randomly selected hippocampal neurons with a smooth and bright appearance and no visible organelles for recording under an inverted microscope (BX51W1, Olympus, Japan). Signals were filtered, amplified, and digitized using a Multi-clamp 700 B amplifier (Molecular Devices, Sunnyvale, CA, USA) and a DigiData 1440A digitizer (Molecular Devices). The data were recorded and analyzed using the pClamp 10.1 software (Molecular Devices). The series resistance was compensated for 85–90%. Recordings were discarded if the series resistance was over 20 M Ω or changed by over 20% during the experiments.

For recording the APs, the intracellular solution contained 130 mM KCl, 1 mM CaCl₂, 2 mM MgCl₂·6H₂O, 10 mM EGTA, 10 mM HEPES, and 2 mM Na₂ATP·3H₂O (pH 7.3 with KOH); the extracellular solution contained 130 mM NaCl, 5 mM KCl, 2 mM CaCl₂, 1 mM MgCl₂·6H₂O, 10 mM HEPES, 10 mM glucose (pH 7.4 with NaOH).

For recording I_{Na} , the intracellular solution contained 130 mM CsCl, 1 mM MgCl₂·6H₂O, 10 mM EGTA, 20 mM TEA-Cl, 10 mM HEPES, and 3 mM Na₂ATP·3H₂O (pH 7.3 with CsOH); the extracellular solution contained 125 mM NaCl, 5.4 mM KCl, 2 mM CaCl₂, 2 mM MgCl₂·6H₂O, 10 mM HEPES, 10 mM glucose, 0.2 mM CdCl₂, 4 mM 4-AP, and 20 mM TEA-Cl (pH 7.4 with NaOH).

For recording K_v currents, the intracellular solution contained 140 mM KCl, 1 mM MgCl₂·6H₂O, 10 mM EGTA, 10 mM HEPES, and 4 mM Na₂ATP·3H₂O (pH 7.3 with KOH); the extracellular solution contained 145 mM NaCl, 5.4 mM KCl, 2 mM CaCl₂, 2 mM MgCl₂·6H₂O, 10 mM HEPES, 10 mM glucose, 0.2 mM CdCl₂, and 0.001 mM tetrodotoxin (pH 7.4 with NaOH). In addition, 20 mM TEA-Cl and 4 mM 4-AP were used to block I_{DR} and I_A , respectively.

To eliminate the influence of neuronal size, we normalized the currents to the cell membrane capacitance to calculate current densities (pA/pF).

Data analysis and statistics

The experimental results were analyzed using Clampfit 10.3 (Molecular Devices), Origin 8.5, and SPSS version 20. Statistical comparisons among the groups were performed using one-way analysis of variance. All data are presented as means \pm SEMs. Statistical significance was set at p-values of <0.05 and extreme significance at p-values of <0.01.

Results

TPEN attenuates A β_{25-35} -induced hippocampal neuronal death

To investigate the effect of TPEN on A β_{25-35} -induced neurotoxicity, we performed a MTT assay to determine hippocampal neuronal death induced by A β_{25-35} . As shown in Fig. 1, exposure of hippocampal neurons to A β_{25-35} at 20 μ M for 24 h induced significant neuronal death (A β_{25-35} treatment vs. control: 64.02 \pm 1.04% vs. 100.00 \pm 1.07%, $p < 0.01$). However, the neuronal death induced by A β_{25-35} was markedly attenuated by treatment with TPEN in a concentration-dependent manner, although it cannot be completely prevented; further, 100 nM of TPEN increased the neuronal viability to 76.98 \pm 1.53%, yielding the best protective effect. Therefore, 100 nM TPEN was used in the subsequent experiments.

TPEN prevented A β_{25-35} -induced intracellular Zn²⁺ concentration increase

We performed single live-cell confocal imaging to investigate the concentration of intracellular Zn²⁺ in primary hippocampal neurons using FluoZin-3, a cell-permeant Zn²⁺-selective fluorescent indicator. We found that the free Zn²⁺ concentration in the control hippocampal neurons was very low (Fig. 2a); however, the Zn²⁺ concentration in the neurons treated with A β_{25-35} markedly increased (Fig. 2b), and TPEN treatment significantly

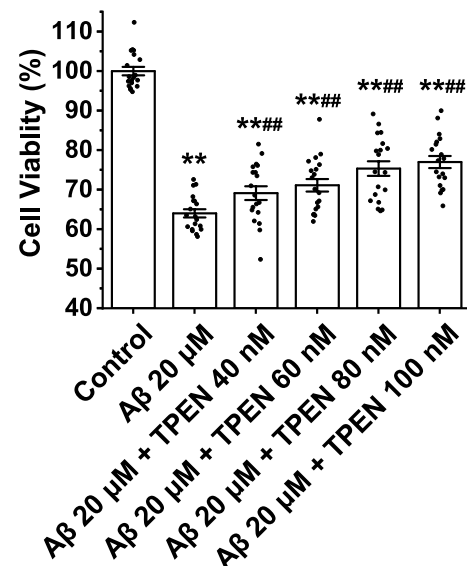
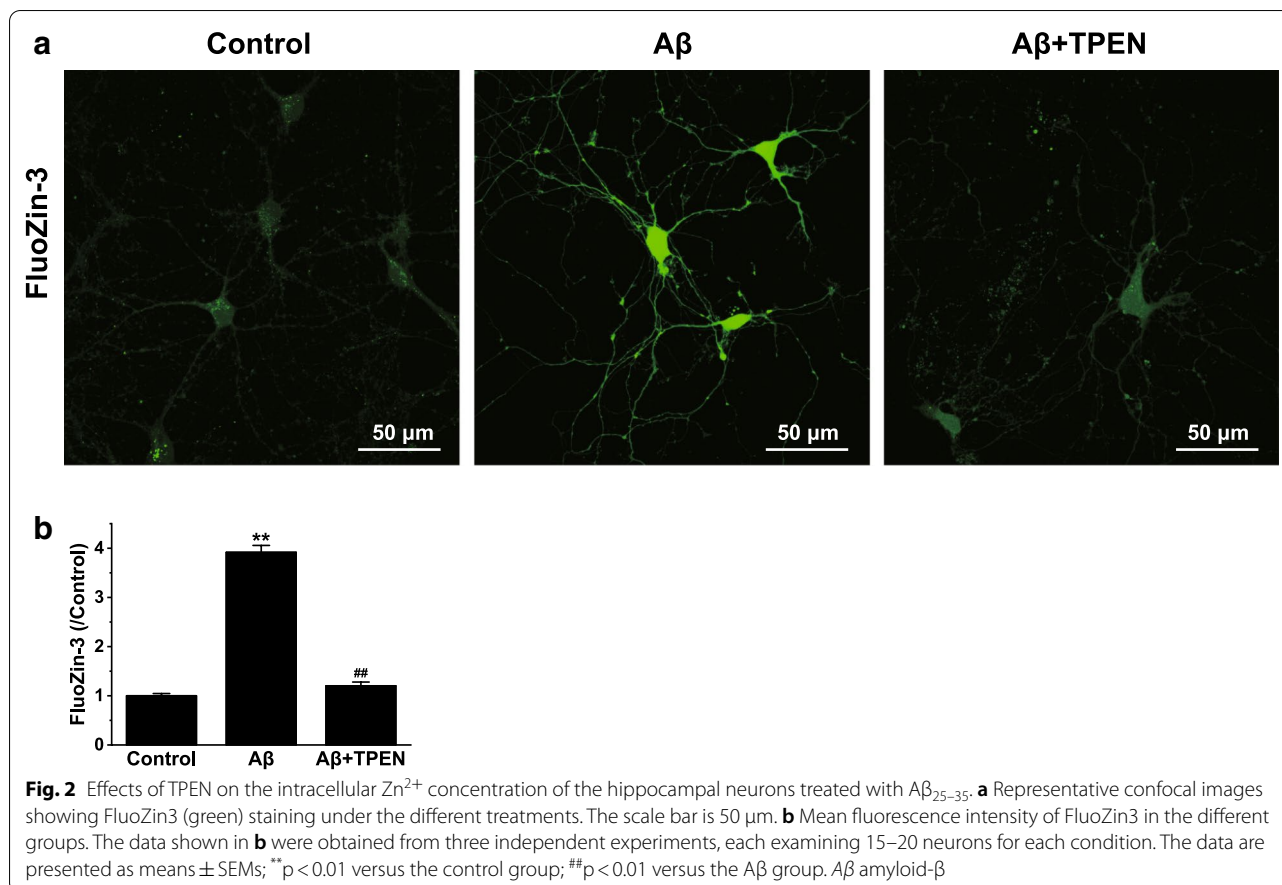


Fig. 1 Effects of TPEN on the viability of the hippocampal neurons treated with A β_{25-35} . The data are presented as means \pm SEMs; ** $p < 0.01$ versus the control group; ### $p < 0.01$ versus the A β group; $n = 19$. A β amyloid- β



reversed the $A\beta_{25-35}$ -induced intracellular Zn^{2+} concentration increase (Fig. 2b). There was no difference between the $A\beta$ + TPEN and control groups ($p > 0.05$).

Effects of TPEN on the frequency of APs in the $A\beta_{25-35}$ -treated hippocampal neurons

The evoked APs were examined by using whole-cell current-clamp recordings, and the repetitive firings were evoked by a 500-ms prolonged depolarizing current injection of 50-pA (Fig. 3a). The results showed that $A\beta_{25-35}$ treatment markedly increased the frequency of APs ($A\beta$ vs. control, $p < 0.01$; Fig. 3b). However, TPEN treatment completely reversed the $A\beta_{25-35}$ -induced the frequency of APs increase ($A\beta$ + TPEN vs. $A\beta$, $p < 0.05$; $A\beta$ + TPEN vs. control, $p > 0.05$; Fig. 3b).

Effects of TPEN on the electrophysiological properties of Na_v in the $A\beta_{25-35}$ -treated hippocampal neurons

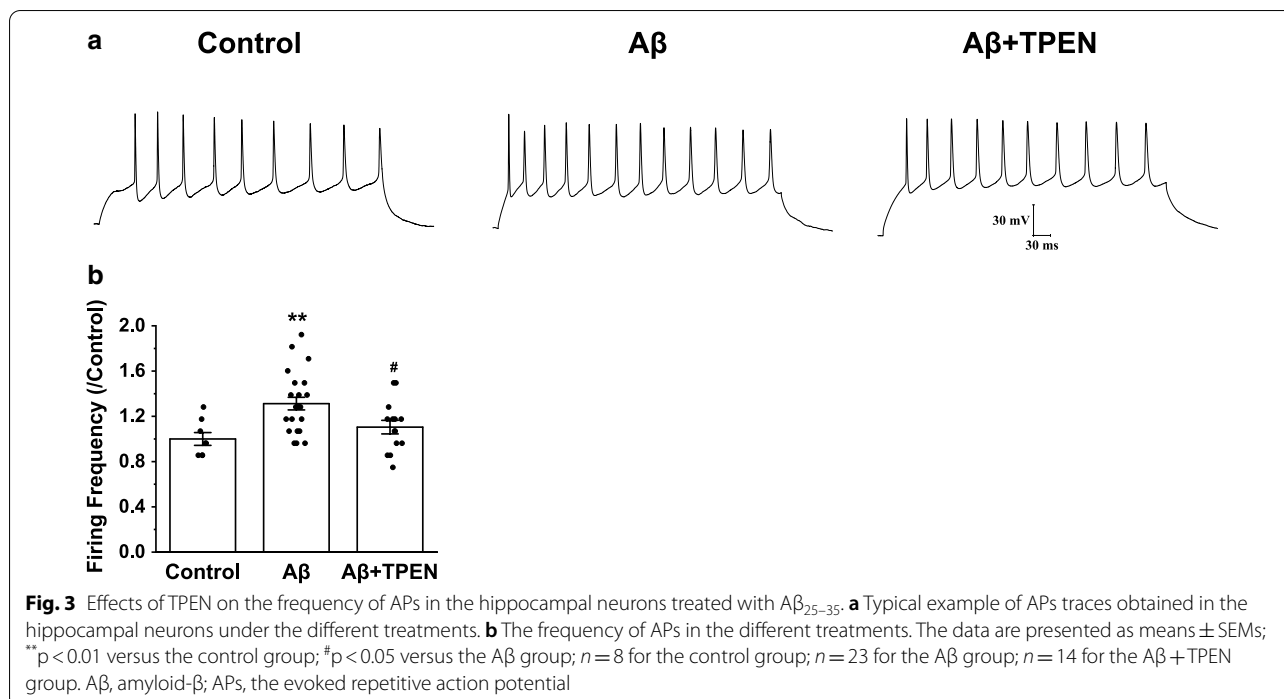
Figures 4, 5, 6 show the properties of Na_v in the hippocampal neurons subjected to the different treatments.

To record Na_v currents (I_{Na}), we held the hippocampal neuron potentials at -80 mV and evoked the current traces using a 20-ms constant depolarizing pulse

from -80 to $+65$ mV in increments of 5 mV (Fig. 4a). Consequently, $A\beta_{25-35}$ significantly increased the maximum current density of I_{Na} compared to the control (from -83.30 ± 5.04 pA/pF to -121.06 ± 11.55 pA/pF, $p < 0.01$; Fig. 4b). Furthermore, the I_{Na} increased at different membrane potentials after exposure to $A\beta$, which were visible from current–voltage (I–V) curves (Fig. 4c), compared to that after exposure to the control ($p < 0.05$). However, pretreatment with TPEN not only completely reversed the increase in the maximum I_{Na} current density caused by $A\beta_{25-35}$ but also prevented the $A\beta_{25-35}$ -induced downward shift of the I–V curves ($A\beta$ + TPEN vs. $A\beta$, $p < 0.05$; $A\beta$ + TPEN vs. control, $p > 0.05$; Fig. 4b, c).

To examine the gating properties of Na_v , we obtained the activation curve of I_{Na} by fitting the Boltzmann equation: $G/G_{Max} = 1/\{1 + \exp[(V_m - V_{1/2})/k]\}$, where $V_{1/2}$ is the half-activation potential and k is the slope factor. The results indicated that there was no significant difference in the activation curve of I_{Na} among all groups (Fig. 4d–f, $p > 0.05$).

To explore the steady-state inactivation kinetics of Na_v , we held the hippocampal neuron potentials



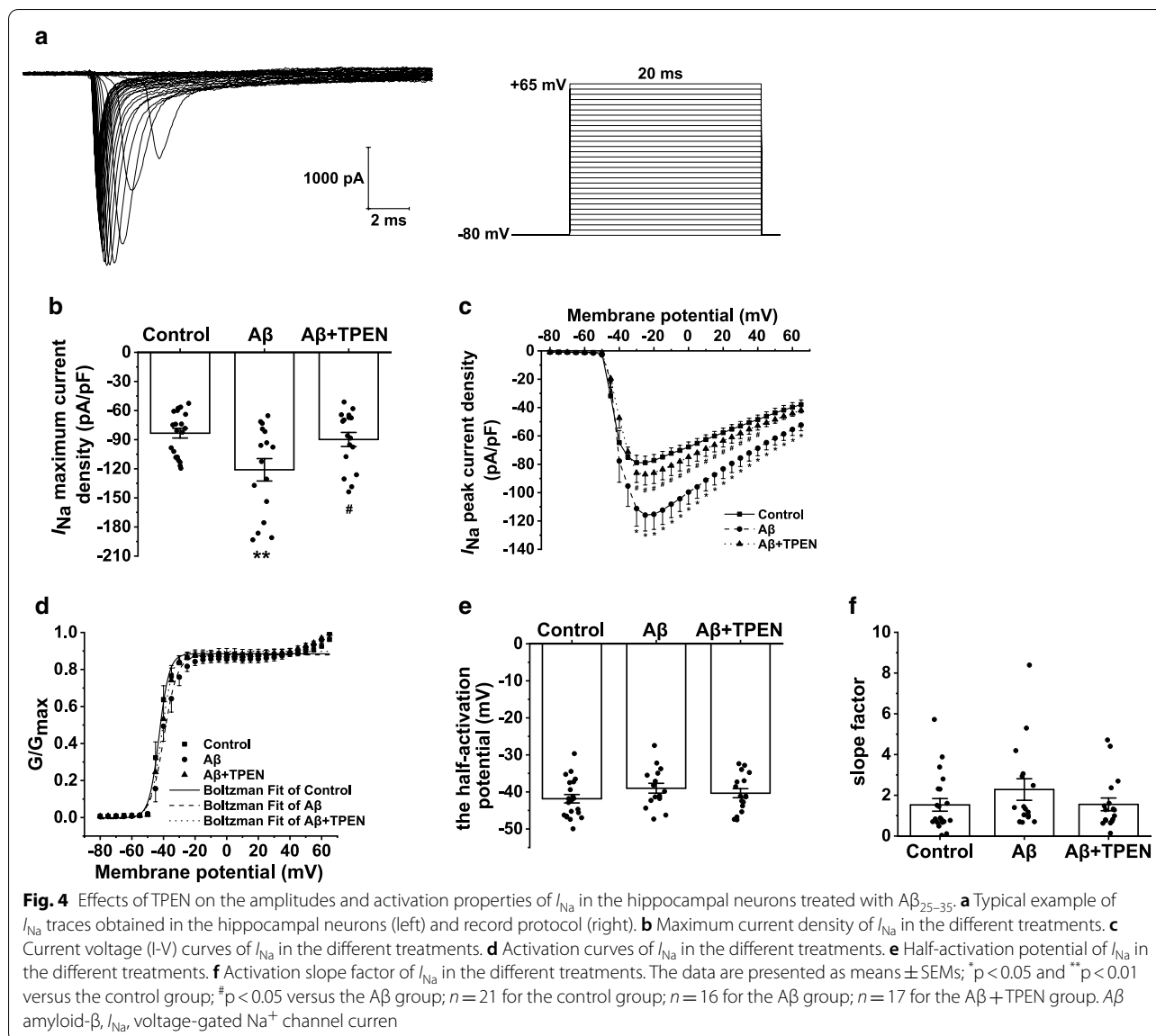
at -90 mV and applied a 60-ms constant depolarizing pulse from -90 to $+100$ mV in increments of 5 mV. The neurons were then treated with a test pulse of -20 mV (20-ms duration; Fig. 5a). The inactivation curves were fitted with the Boltzmann equation: $I/I_{Max} = 1/\{1 + \exp[(V_m - V_{1/2})/k]\}$, where $V_{1/2}$ is the half-inactivation potential and k is the slope factor. A β_{25-35} treatment resulted in hyperpolarization of Na_v and significantly decreased the $V_{1/2}$ (A β vs. control, $p < 0.01$; Fig. 5b, c). TPEN treatment markedly reversed the A β_{25-35} -induced effects (A β + TPEN vs. A β , $p < 0.01$; A β + TPEN vs. control, $p > 0.05$). However, there were no significant changes in k in all groups (Fig. 5d).

To examine the kinetics of recovery from inactivation of Na_v , we held the hippocampal neuron potentials at -90 mV and applied a depolarizing pulse of -10 mV (15-ms duration). The neurons were then treated with a test pulse of -10 mV (15-ms duration) after a series of -90 -mV intervals varying from 0.5 to 44.5 ms (Fig. 6a). The recovery curve of Na_v from inactivation was fitted with the monoexponential equation: $I/I_{Max} = 1 - \exp(-\Delta t/\tau)$, where τ is the time constant. The results indicated that A β_{25-35} did not alter the recovery characteristics after Na_v inactivation. There was no significant difference in the recovery time constant from inactivation of Na_v among all groups (Fig. 6b, c).

Effects of TPEN on the electrophysiological properties of I_A in the A β_{25-35} -treated hippocampal neurons

The hippocampal neuron potentials were held at -90 mV, and the current traces were evoked using a 200-ms constant depolarizing pulse from -80 to $+100$ mV in increments of 10 mV (Fig. 7a). To isolate I_A , we used tetraethylammonium chloride (TEA-Cl, 20 mM) to block the I_{DR} . Compared with that in the control group, the maximum I_A current density in the A β_{25-35} group significantly decreased from 155.61 ± 7.41 pA/pF to 62.08 ± 2.50 pA/pF ($p < 0.01$; Fig. 7b). Furthermore, A β_{25-35} treatment markedly reduced I_A at different membrane potentials, which were visible from the I-V curves (Fig. 7c), compared to the control ($p < 0.01$). However, TPEN treatment significantly inhibited the decrease in the maximum I_A current density and downward shift of the I-V curves caused by A β_{25-35} , although these changes were not completely prevented (A β + TPEN vs. A β , $p < 0.01$; A β + TPEN vs. control, $p < 0.01$; Fig. 7b, c).

The activation curve of I_A was obtained by fitting the Boltzmann equation: $I/I_{Max} = 1/\{1 + \exp[(V_m - V_{1/2})/k]\}$, where $V_{1/2}$ is the half-activation potential and k is the slope factor. The results indicated that the activation curve of I_A shifted to hyperpolarization, and the $V_{1/2}$ significantly decreased (A β vs. control, $p < 0.05$) after A β_{25-35} treatment (Fig. 7d, e). TPEN inhibited the $V_{1/2}$ decrease induced by A β_{25-35} (A β + TPEN vs. A β , $p < 0.05$; A β + TPEN vs. control,

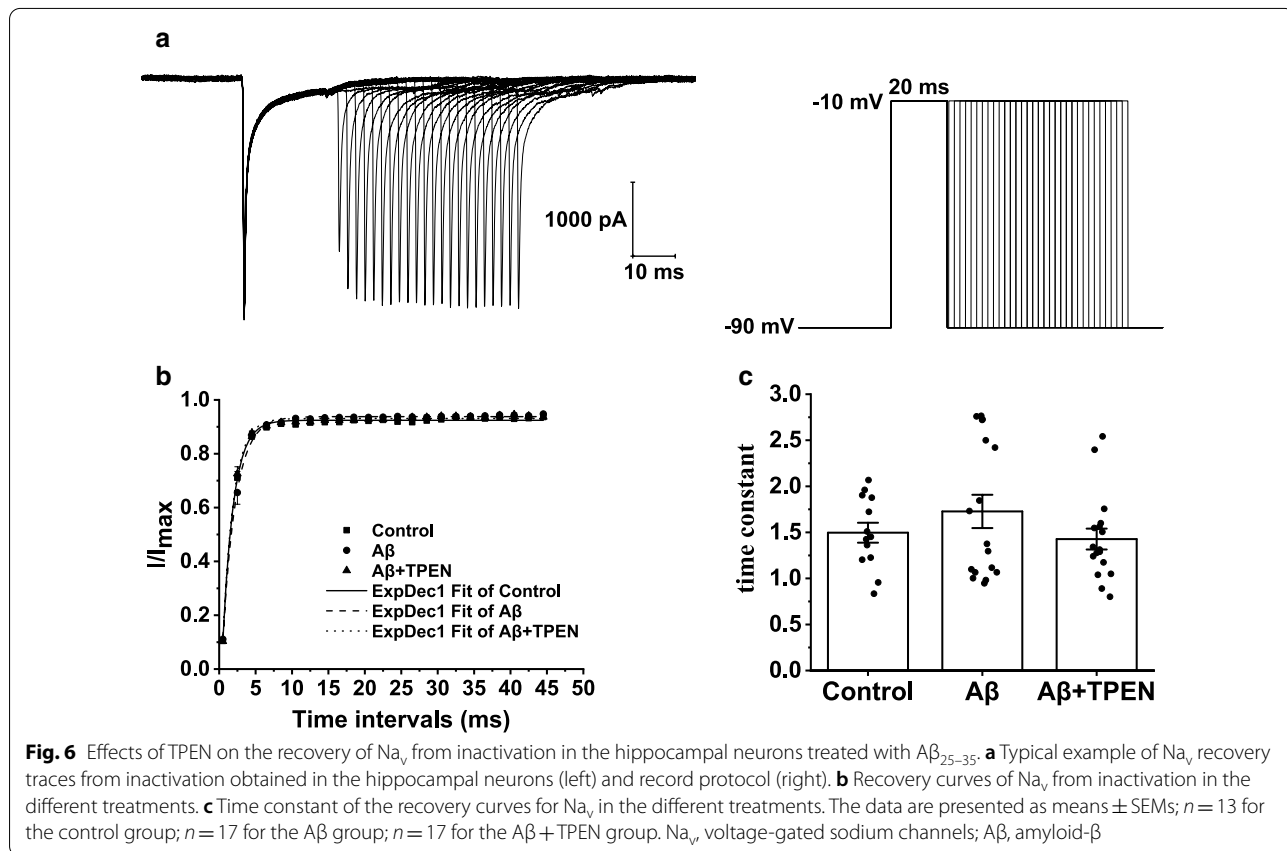
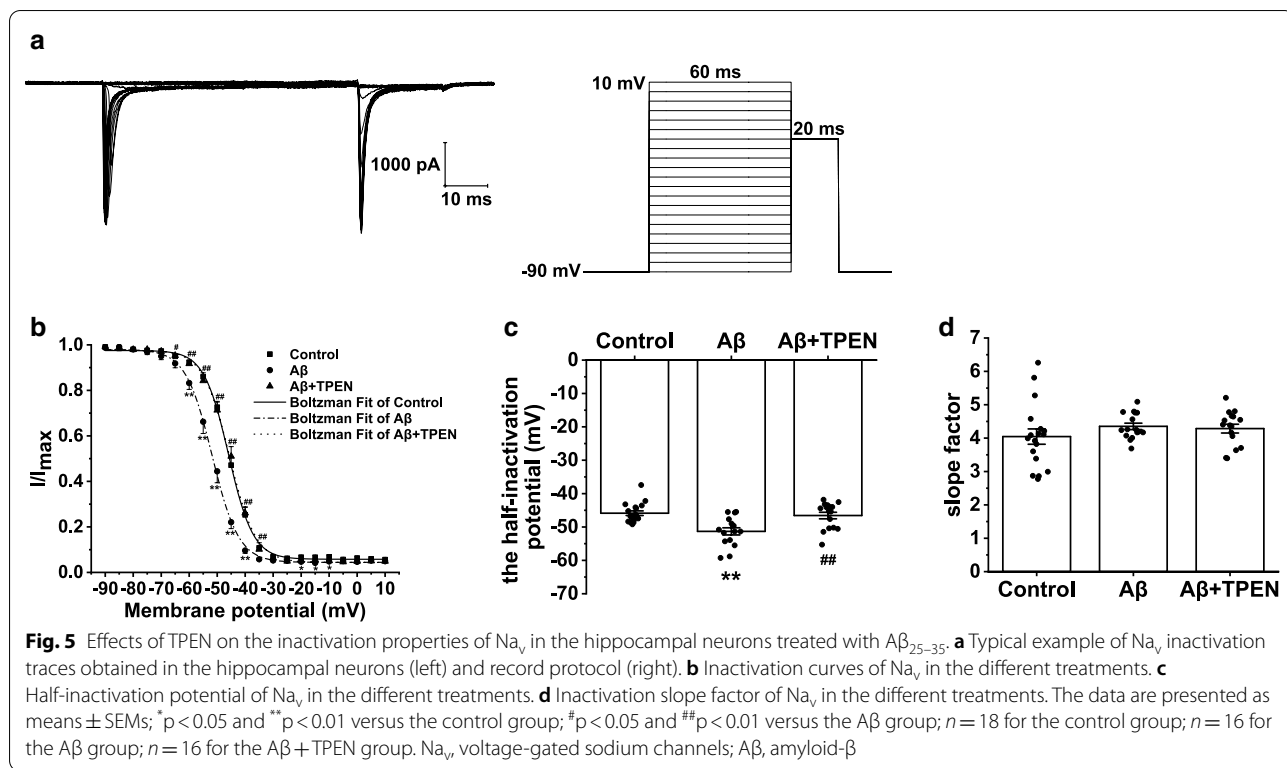


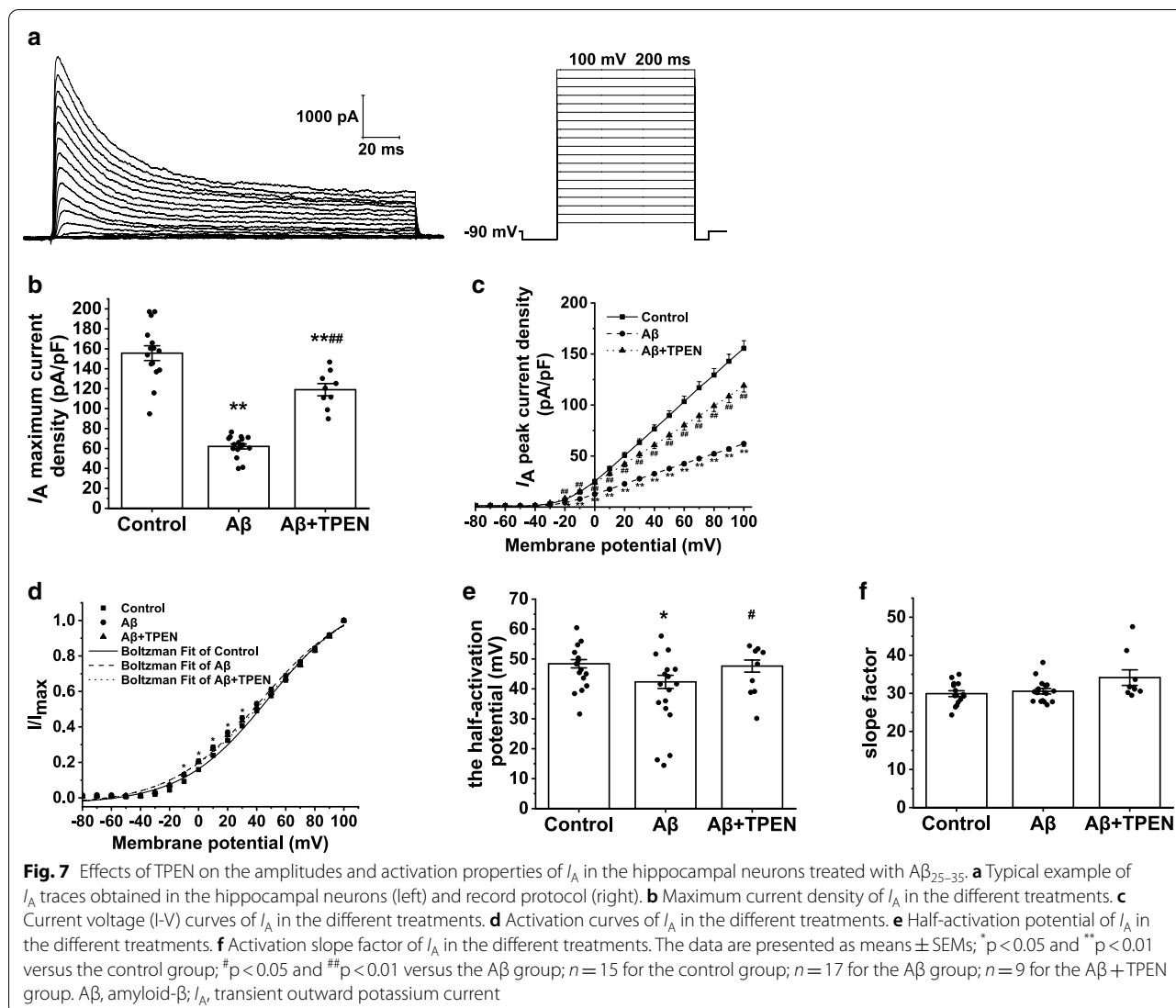
$p > 0.05$; Fig. 7d, e). However, there was no significant difference found in k between the groups (Fig. 7f).

To explore the steady-state inactivation kinetics of I_A , we held the hippocampal neuron potentials at -90 mV and applied an 80-ms constant depolarizing pulse from -120 to $+10$ mV in increments of 10 mV. The neurons were then treated with a test pulse of 50 mV (80-ms duration) (Fig. 8a). The inactivation curves were fitted using the Boltzmann equation: $I/I_{Max} = 1 / \{1 + \exp[(V_m - V_{1/2})/k]\}$, where $V_{1/2}$ is the half-inactivation potential and k is the slope factor. Compared to those in the control, the inactivation curves in the $A\beta_{25-35}$ group shifted to hyperpolarization (Fig. 8b). Moreover, $A\beta_{25-35}$ treatment significantly reduced the $V_{1/2}$ and k ($A\beta$ vs. control, $p < 0.01$; Fig. 8c,

d). TPEN treatment reversed the $V_{1/2}$ and k decreases caused by $A\beta_{25-35}$ ($A\beta + TPEN$ vs. $A\beta$, $p < 0.01$; $A\beta + TPEN$ vs. control, $p > 0.05$; Fig. 8c, d).

To examine the kinetics of recovery from I_A activation, we held the hippocampal neuron potentials at -90 mV and applied a depolarizing pulse of 50 mV (50-ms duration). The neurons were then treated with a test pulse of 50 mV (50-ms duration) following a series of -90 -mV intervals varying from 5 to 290 ms (Fig. 9a). The recovery curve of I_A from inactivation was fitted with the monoexponential equation: $I/I_{Max} = 1 - \exp(-\Delta t/\tau)$, where τ is the time constant. The results showed that $A\beta_{25-35}$ treatment markedly increased the time constant ($A\beta$ vs. control, $p < 0.01$; Fig. 9b, c). However, TPEN treatment completely





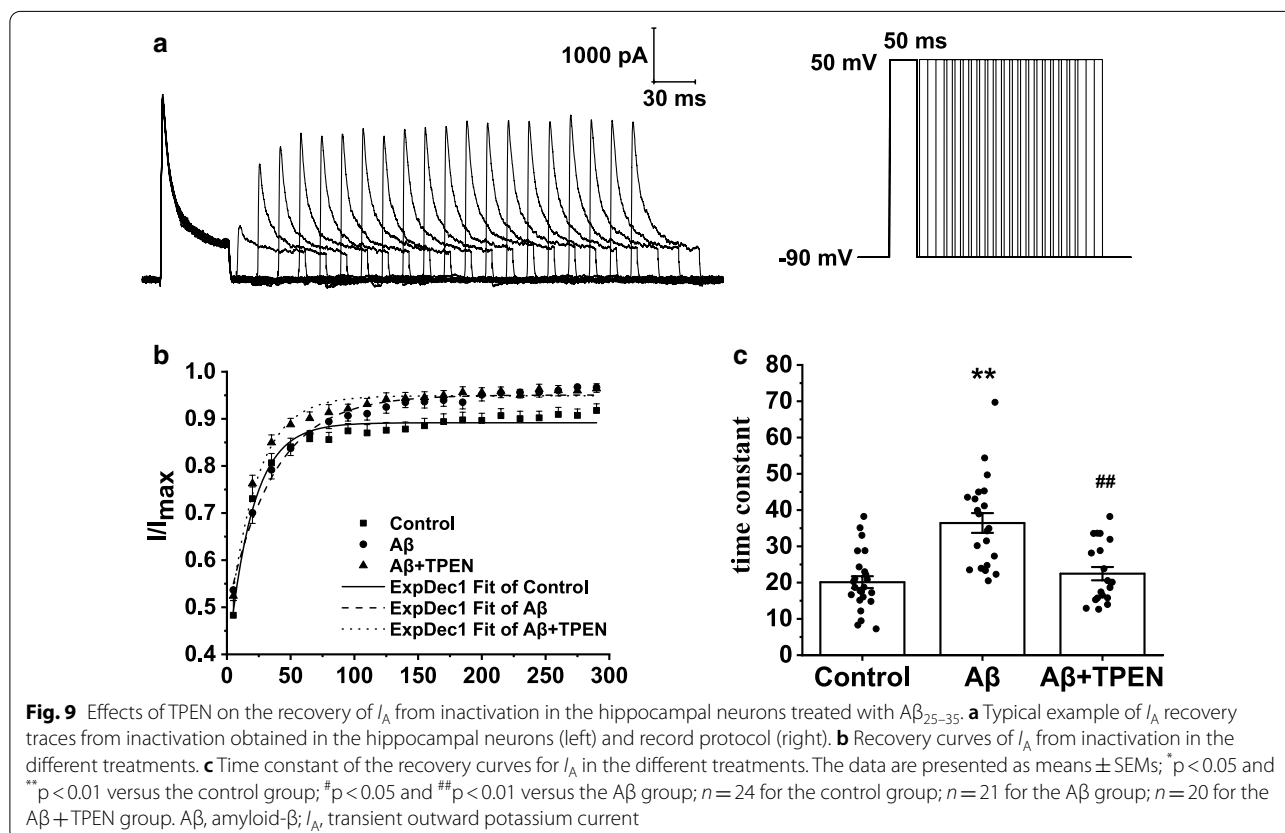
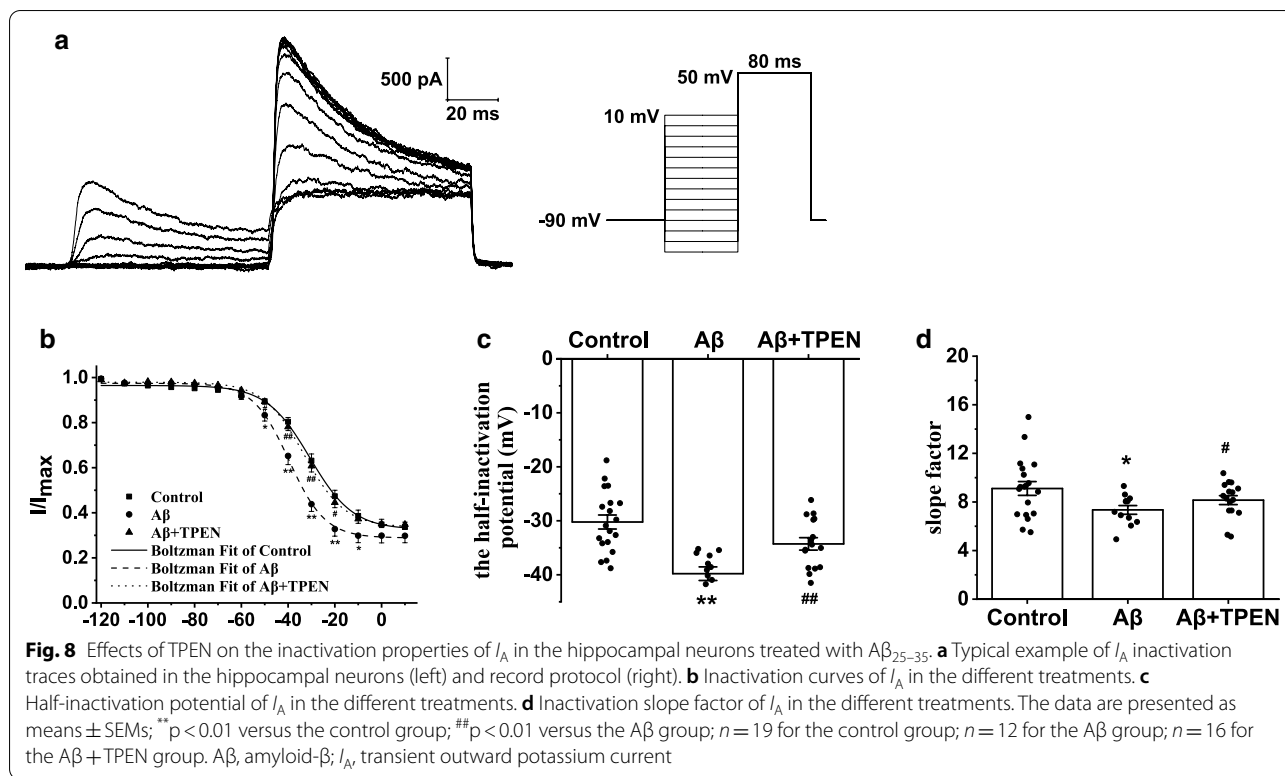
reversed the $A\beta_{25-35}$ -induced recovery time constant increase ($A\beta$ + TPEN vs. $A\beta$, p < 0.01; $A\beta$ + TPEN vs. control, p > 0.05; Fig. 9b, c).

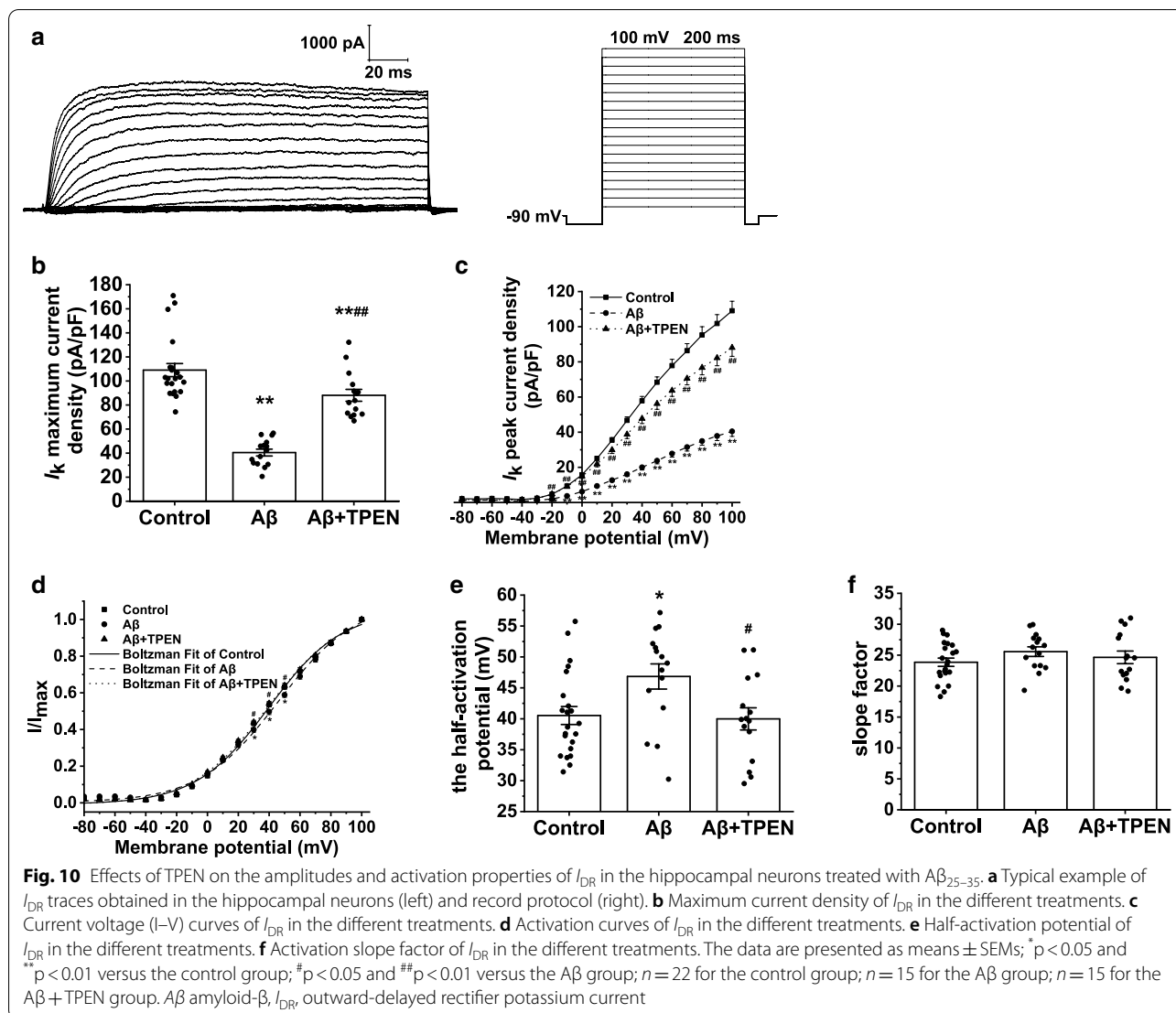
Effects of TPEN on the electrophysiological properties of I_{DR} in the $A\beta_{25-35}$ -treated hippocampal neurons

To investigate the properties of I_{DR} in the hippocampal neurons subjected to the different treatments, we held the hippocampal neuron potentials at -90 mV and evoked the current traces using a 200-ms constant depolarizing pulse from -80 to $+100$ mV in increments of 10 mV (Fig. 10a). To isolate I_{DR} , we used 4-aminopyridine (4-AP; 4 mM) to block the I_A . After incubation with $A\beta_{25-35}$, the maximum current density of I_{DR} significantly decreased compared to that in the control group (from 109.06 ± 5.44 pA/pF to 40.45 ± 2.86 pA/pF, p < 0.01; Fig. 10b). The maximum I_{DR} current density in

the $A\beta_{25-35}$ + TPEN group was 88.07 ± 4.92 pA/pF; this treatment significantly alleviated the reduction caused by $A\beta_{25-35}$, and a significant difference was still found compared with that in the control group ($A\beta$ + TPEN vs. $A\beta$, p < 0.01; $A\beta$ + TPEN vs. control, p < 0.01; Fig. 10b). Furthermore, as shown in the I - V curves, $A\beta_{25-35}$ treatment decreased I_{DR} at different membrane potentials compared to the control ($A\beta$ vs. control, p < 0.01), whereas TPEN pretreatment significantly alleviated this effect induced by $A\beta_{25-35}$ ($A\beta$ + TPEN vs. $A\beta$, p < 0.01; Fig. 10c).

The activation curve of I_{DR} was obtained by fitting the Boltzmann equation: $I/I_{Max} = 1/[1 + \exp[(V_m - V_{1/2})/k]]$, where $V_{1/2}$ is the half-activation potential and k is the slope factor. After $A\beta_{25-35}$ treatment, the activation curves of I_{DR} shifted to depolarization, and the $V_{1/2}$ significantly increased





($A\beta$ vs. control, $p < 0.05$; Fig. 10d, e). TPEN markedly reversed these changes caused by $A\beta_{25-35}$ ($A\beta + TPEN$ vs. $A\beta$, $p < 0.01$; $A\beta + TPEN$ vs. control, $p > 0.05$; Fig. 10d, e). Additionally, k in the $A\beta_{25-35}$ group showed an upward trend; however, there was no significant difference in k among all groups (Fig. 10f).

Discussion

This study showed that TPEN attenuated $A\beta_{25-35}$ -induced neuronal death, reversed $A\beta_{25-35}$ -induced intracellular Zn^{2+} concentration and the frequency of APs increase, inhibited $A\beta_{25-35}$ -induced maximum current density increase in I_{Na} , and relieved $A\beta_{25-35}$ -induced decrease in the peak amplitudes of I_A and I_{DR} at different membrane potentials. These results suggested that $A\beta_{25-35}$ -induced neuronal damage correlated with Zn^{2+}

dysregulation mediated the electrophysiological changes in Na_v and K_v .

As an important neuromodulator in the brain, Zn^{2+} is involved in brain development and neural function. Under physiological conditions, the basal extracellular Zn^{2+} level in the hippocampus is in the low nanomolar (~ 10 nM) range and increases age-dependently [37, 38]. Extracellular Zn^{2+} is released from the synaptic vesicles of glutamatergic neurons (zincergic neurons) during synaptic activity, which plays an important role in regulating synaptic transmission and plasticity [39, 40]. The basal intracellular Zn^{2+} level is much lower (~ 100 pM) than the extracellular Zn^{2+} level, and impaired intracellular Zn^{2+} homeostasis has been implicated in AD pathogenesis [41]. When the $A\beta$ concentration in the extracellular compartment reaches a high level (> 100 pM), $A\beta$ can rapidly bind to extracellular Zn^{2+} with high affinity

through histidine residues [17, 42]. The Zn-A β complexes formed in the extracellular compartment would be rapidly taken up into presynaptic and postsynaptic neurons. Free Zn²⁺ can be released from Zn-A β complexes, causing an increase in intracellular Zn²⁺ and A β concentrations, leading to neuronal death and cognitive decline [17, 43]. Moreover, owing to the age-related increase in extracellular Zn²⁺, A β -induced intracellular Zn²⁺ toxicity is accelerated with aging [43]. Furthermore, long-term potentiation was not changed by perfusion with 1 000 nM A β but was markedly attenuated by perfusion with 5 nM A β in the presence of extracellular Zn²⁺ (10 nM), indicating that extracellular Zn²⁺ is essential for A β -induced cognitive decline [17]. Additionally, the weakened capacity of the intracellular Zn²⁺-buffering system also contributes to A β -induced intracellular Zn²⁺ dysregulation in AD. The expression of zinc transporter-3 protein and the Zn²⁺ binding protein (metallothioneins 3, MT-III) decreased in the AD brain [44–46]. Conversely, excess extracellular calcium (Ca²⁺) influx into postsynaptic neurons through N-methyl-D-aspartate receptors leads to glutamate excitotoxicity, which is a common pathway for neuronal death and hippocampal neurodegeneration in AD pathogenesis [47]. However, extracellular Zn²⁺ can pass through Ca²⁺- and Zn²⁺-permeable N-methyl-D-aspartate receptors, voltage-gated Ca²⁺ channels, and GluR2-lacking α -amino-3-hydroxy-5-methyl-4-isoxazolepropionate receptors [48]. Excess influx of extracellular Zn²⁺ is more likely to contribute to glutamate excitotoxicity than is the influx of extracellular Ca²⁺, because the intracellular Zn²⁺ concentration (~100 pM) is much lower than the intracellular Ca²⁺ concentration (~100 nM) but has higher neurotoxicity [49–52]. These data indicate that it is important to prevent A β -induced neurotoxicity and cognitive decline by maintaining intracellular Zn²⁺ homeostasis. Herein, exposure of primary hippocampal neurons to 20 μ M A β_{25-35} for 24 h significantly decreased neuronal viability and increased the intracellular Zn²⁺ concentration, whereas TPEN, a membrane-permeable Zn²⁺-specific chelator, attenuated A β_{25-35} -induced neuronal death and reversed A β_{25-35} -induced intracellular Zn²⁺ concentration increase. Coincidentally, Yang et al. recently reported that treatment with A β_{25-35} increased intracellular Zn²⁺, then might cause mitochondrial depolarization, formation of ROS, the activation of caspase-3, and neuron damage in cultured rat hippocampal neurons, also suggesting synergy neurotoxic effects of intracellular Zn²⁺ and amyloid beta [53]. Taken together, intracellular Zn²⁺ dysregulation mediated the neurotoxicity of A β_{25-35} , and it may be an effective strategy for preventing A β -induced neuronal damage by capturing Zn²⁺ released from intracellular Zn-A β complexes.

As mentioned above, hippocampal neuronal hyperexcitability and abnormal neuronal activity contribute to cognitive decline in AD, and excess extracellular Zn²⁺ influx is involved in Glu-associated excitotoxicity in AD pathogenesis. Action potential (AP) is the basic characteristic reflecting neuronal excitability on mammalian central nervous system, which is regulated by ion channels in membrane [54]. Some evidence suggests that Na_v, a key regulator of neuronal excitability, is involved in AD-related hippocampal pathological hyperactivity [29]. Soluble A β may induce neuronal hyperexcitation by increasing the amplitude of Na⁺ currents [26]. However, the connection between A β -induced intracellular Zn²⁺ dysregulation and changes in Na_v properties remains unclear. After observing the protective effect of TPEN on the neurotoxicity caused by A β herein, we investigated the involvement mechanism of TPEN neuroprotection aimed at A β based on electrophysiological properties. Our study demonstrated that soluble A β_{25-35} markedly increased the frequency of APs and the maximum current density of I_{Na} , significantly elevated I_{Na} at different membrane potentials. Moreover, soluble A β_{25-35} induced the inactivation curves to significantly shift to hyperpolarization, indicating that I_{Na} can be inactivated more easily. Taken together, the pathologically related soluble A β levels increased the excitability of the primary hippocampal neurons in vitro. However, TPEN treatment largely reversed the changes in the electrophysiological properties of APs and Na_v caused by A β_{25-35} . These results suggested that intracellular Zn²⁺ dysregulation may be involved in A β -induced changes in Na_v, leading to hippocampal excitability impairment.

K_v plays a significant role in maintaining the resting membrane potential and regulating cell excitability, becoming a potential therapeutic target for the treatment of neurodegenerative diseases [55]. Based on the current characteristics, K_v can be divided into I_A and I_{DR} [56]. I_A mainly contributes to neuronal repolarization and repetitive firing of the action potential and is characterized by rapid activation and inactivation [32, 57]. I_{DR} mainly regulates the process of repolarization in neurons and has the characteristics of delayed long-lasting activation and non-inactivation [32, 57]. Inhibiting I_A and I_{DR} can increase the excitability of rat hippocampal neurons [32]. Moreover, the expression and functional alterations of K_v may be related to the neuronal hyperexcitability caused by A β , contributing to AD progress and development [31]. Herein, we observed that the maximum current density and I–V curves of I_A and I_{DR} significantly decreased after A β_{25-35} exposure. Moreover, both the steady-state activation and inactivation curves of I_A significantly shifted toward hyperpolarization upon A β_{25-35} treatment, which implied that the voltage sensitivity of

activation and inactivation was reduced. Besides, $A\beta_{25-35}$ obviously elevated the recovery time from inactivation, suggesting that I_A took a longer time to open again after inactivation. These results indicated that $A\beta_{25-35}$ had a significant inhibitory effect on the I_A and I_{DR} of the hippocampal neurons, leading to increased hippocampal neuronal excitability. Further, TPEN significantly restored the changes in the electrophysiological properties of I_A and I_{DR} caused by $A\beta_{25-35}$, which suggested that $A\beta_{25-35}$ induced the excessive influx of intracellular Zn^{2+} , changing the electrophysiological characteristics of K_v . In fact, the excitability of cultured mouse hippocampal neurons increased in the presence of exogenous Zn^{2+} (50 μ M) by increasing the firing frequency and inhibiting I_A [58]. Furthermore, similar results were found in dopaminergic neurons of the rat substantia nigra and rat cardiomyocytes [59–61]. The mRNA levels of $K_v1.4$ and $K_v4.3$, which are the major components of I_A , markedly decreased in rat cardiomyocytes with a high concentration of intracellular Zn^{2+} (100 nM) [61, 62]. These observations suggest that the neurotoxicity of $A\beta$ may be, at least partially, attributed to the increase in intracellular Zn^{2+} caused by $A\beta$, which inhibits K_v activity; and TPEN could attenuate this excitability impairment via recovering potassium currents.

The existed studies suggest that abnormal Zn^{2+} homeostasis be the cause of a variety of health problems [48], for example, in hypoxic–ischemic conditions, TPEN, a specific free Zn^{2+} chelator could inhibit neuronal death by modulating apoptosis, glutamate signaling, and voltage-gated K^+ and Na^+ channels in neurons [63]. TPEN also could increase the survival rate of retinal ganglion cells and promote considerable axon regeneration after the optic nerve injury [64, 65]. Moreover, TPEN induced pancreatic cancer cell death through increasing oxidative stress and restraining cell autophagy [66]. Our study also suggest that maintaining intracellular Zn^{2+} homeostasis be also an effective program to alleviate $A\beta$ -induced neuronal damage in AD. And TPEN might represent a potential cell-targeted therapy in Zn^{2+} -related diseases. However, most studies including our present study currently focused on cells and animals experiments applying TPEN. To solve some involved human diseases applying TPEN, we should implement some human studies applying TPEN with a step-by-step after more animal experiments.

In conclusion, our study demonstrated that $A\beta_{25-35}$ -induced neuronal death was correlated with intracellular Zn^{2+} dysregulation, which markedly changed the electrophysiological properties of Na_v and K_v , including the obvious increase in Na_v activities and noticeable decrease in I_A and I_{DR} activities in the primary hippocampal neurons. TPEN attenuated $A\beta_{25-35}$ -induced neuronal death

by recovering intracellular Zn^{2+} concentrations and the electrophysiological properties of Na_v and K_v . Maintaining intracellular Zn^{2+} homeostasis may be an effective program to alleviate $A\beta$ -induced neuronal damage in AD. However, the deep mechanisms of intracellular Zn^{2+} or abnormal Zn^{2+} homeostasis on the activities of Na_v and K_v channels changes needs to be further studied. Furthermore, the result in present study only was from in vitro experiment applying cultured neurons, it needs more animals and human studies to conform the role of TPEN, a specific free Zn^{2+} chelator in neurodegenerative diseases including AD. If so, TPEN, a specific free Zn^{2+} chelator might be developed as drug against neurodegenerative diseases including AD.

Acknowledgements

The authors acknowledge the support provided by National Natural Science Foundation of China and Natural Science Foundation of Tianjin City, china. We would like to thank Editage (www.editage.cn) for English language editing.

Authors' contributions

WBC designed and performed the experiments, analyzed the experimental data, prepared all figures, and wrote the manuscript. YQL conceived the study, reviewed and revised the manuscript. The other authors help to perform the experiments, collect experimental data, review and revise the manuscript, and apply the funds. All authors read and approved the final manuscript.

Funding

This work was supported by grants from the National Natural Science Foundation of China (31272317), the National Nature Science Youth Foundation of China (81801076), the Natural Science Foundation of Tianjin City (20JCYBJC01370), Natural Science Foundation of Tianjin City (15JCYBJC24500), the Tianjin Natural Science Youth Foundation (18JCQNJC11400), the Fundamental Research Funds for the Central Universities of Nankai University (BE123081), and Scientific Research Project of Hebei Province Administration of Traditional Chinese Medicine (No. 2020143).

Availability of data and materials

The data that support the findings of this study are available from the corresponding author upon reasonable request.

Code availability

Not applicable.

Declarations

Ethics approval and consent to participate

All procedures were compliant with the approved protocol from the Animal Ethics Committee of Nankai University and the Chinese animal welfare act and the "Chinese code of practice and use of animals for scientific purposes."

Consent for publication

Not applicable.

Competing interests

The authors declare that they have no competing interests.

Author details

¹College of Life Sciences, Nankai University, Tianjin 300071, People's Republic of China. ²Department of Immunology and Pathogenic Biology, School of Basic Medical Sciences, Hebei University of Chinese Medicine, Shiji-azhuang 050200, Hebei, People's Republic of China. ³Tianjin Key Laboratory of Cerebral Vascular and Neurodegenerative Diseases, Tianjin Neurosurgery Institute, Department of Neurology, Tianjin Huanhu Hospital Affiliated to Nankai University, Tianjin, People's Republic of China.

Received: 5 May 2021 Accepted: 2 August 2021
Published online: 12 August 2021

References

- Hardy J, Selkoe DJ. The amyloid hypothesis of Alzheimer's disease: progress and problems on the road to therapeutics. *Science*. 2002;297(5580):353–6.
- Goedert M, Spillantini MG. A century of Alzheimer's disease. *Science*. 2006;314(5800):777–81.
- Mawuenyega KG, Sigurdson W, Ovod V, Munsell L, Kasten T, Morris JC, et al. Decreased clearance of CNS beta-amyloid in Alzheimer's disease. *Science*. 2010;330(6012):1774.
- Praticò D. Oxidative stress hypothesis in Alzheimer's disease: a reappraisal. *Trends Pharmacol Sci*. 2008;29(12):609–15.
- Minkeviciene R, Rheims S, Dobszay MB, Zilberter M, Hartikainen J, Fülöp L, et al. Amyloid beta-induced neuronal hyperexcitability triggers progressive epilepsy. *J Neurosci*. 2009;29(11):3453–62.
- Mucke L, Selkoe DJ. Neurotoxicity of amyloid β -protein: synaptic and network dysfunction. *Cold Spring Harb Perspect Med*. 2012;2(7):006338.
- Zhang Y, Gladyshev VN. Comparative genomics of trace element dependence in biology. *J Biol Chem*. 2011;286(27):23623–9.
- Prasad AS. Impact of the discovery of human zinc deficiency on health. *J Am Coll Nutr*. 2009;28(3):257–65.
- Chasapis CT, Loutsidou AC, Spiliopoulou CA, Stefanidou ME. Zinc and human health: an update. *Arch Toxicol*. 2012;86(4):521–34.
- Shuttleworth CW, Weiss JH. Zinc: new clues to diverse roles in brain ischemia. *Trends Pharmacol Sci*. 2011;32(8):480–6.
- Faller P, Hureau C. Bioinorganic chemistry of copper and zinc ions coordinated to amyloid-beta peptide. *Dalton Trans*. 2009;7:1080–94.
- Takeda A, Tamano H, Hashimoto W, Kobuchi S, Suzuki H, Murakami T, et al. Novel defense by metallothionein induction against cognitive decline: from amyloid β (1–42)-induced excess Zn(2+) to functional Zn(2+) deficiency. *Mol Neurobiol*. 2018;55(10):7775–88.
- Rychlik M, Mlyniec K. Zinc-mediated neurotransmission in Alzheimer's disease: a potential role of the GPR39 in Dementia. *Curr Neuropharmacol*. 2020;18(1):2–13.
- Faller P, Hureau C, Berthoumieu O. Role of metal ions in the self-assembly of the Alzheimer's amyloid- β peptide. *Inorg Chem*. 2013;52(21):12193–206.
- Lovell MA, Robertson JD, Teesdale WJ, Campbell JL, Markesbery WR. Copper, iron and zinc in Alzheimer's disease senile plaques. *J Neurol Sci*. 1998;158(1):47–52.
- Cirrito JR, Yamada KA, Finn MB, Sloviter RS, Bales KR, May PC, et al. Synaptic activity regulates interstitial fluid amyloid-beta levels in vivo. *Neuron*. 2005;48(6):913–22.
- Takeda A, Tamano H, Tempaku M, Sasaki M, Uematsu C, Sato S, et al. Extracellular Zn(2+) is essential for amyloid β (1–42)-induced cognitive decline in the normal brain and its rescue. *J Neurosci*. 2017;37(30):7253–62.
- Tamano H, Takiguchi M, Tanaka Y, Murakami T, Adlard PA, Bush AI, et al. Preferential neurodegeneration in the dentate gyrus by amyloid β (1–42)-induced intracellular Zn(2+) dysregulation and its defense strategy. *Mol Neurobiol*. 2020;57(4):1875–88.
- Tamano H, Oneta N, Shioya A, Adlard PA, Bush AI, Takeda A. In vivo synaptic activity-independent co-uptakes of amyloid β (1–42) and Zn(2+) into dentate granule cells in the normal brain. *Sci Rep*. 2019;9(1):6498.
- Li X, Jiang LH. Multiple molecular mechanisms form a positive feedback loop driving amyloid β 42 peptide-induced neurotoxicity via activation of the TRPM2 channel in hippocampal neurons. *Cell Death Dis*. 2018;9(2):195.
- Vossel KA, Tartaglia MC, Nygaard HB, Zeman AZ, Miller BL. Epileptic activity in Alzheimer's disease: causes and clinical relevance. *Lancet Neurol*. 2017;16(4):311–22.
- Bakker A, Krauss GL, Albert MS, Speck CL, Jones LR, Stark CE, et al. Reduction of hippocampal hyperactivity improves cognition in amnesic mild cognitive impairment. *Neuron*. 2012;74(3):467–74.
- Verret L, Mann EO, Hang GB, Barth AM, Cobos I, Ho K, et al. Inhibitory interneuron deficit links altered network activity and cognitive dysfunction in Alzheimer model. *Cell*. 2012;149(3):708–21.
- Busche MA, Chen X, Henning HA, Reichwald J, Staufenbiel M, Sakmann B, et al. Critical role of soluble amyloid- β for early hippocampal hyperactivity in a mouse model of Alzheimer's disease. *Proc Natl Acad Sci U S A*. 2012;109(22):8740–5.
- Tamagnini F, Scullion S, Brown JT, Randall AD. Intrinsic excitability changes induced by acute treatment of hippocampal CA1 pyramidal neurons with exogenous amyloid β peptide. *Hippocampus*. 2015;25(7):786–97.
- Ren SC, Chen PZ, Jiang HH, Mi Z, Xu F, Hu B, et al. Persistent sodium currents contribute to A β 1–42-induced hyperexcitation of hippocampal CA1 pyramidal neurons. *Neurosci Lett*. 2014;580:62–7.
- Yu FH, Catterall WA. Overview of the voltage-gated sodium channel family. *Genome Biol*. 2003;4(3):207.
- Catterall WA, Goldin AL, Waxman SG. International Union of Pharmacology. XLVII. Nomenclature and structure-function relationships of voltage-gated sodium channels. *Pharmacol Rev*. 2005;57(4):397–409.
- Ciccione R, Franco C, Piccialli I, Boscia F, Casamassa A, de Rosa V, et al. Amyloid β -induced upregulation of Na(v)16 underlies neuronal hyperactivity in Tg2576 Alzheimer's disease mouse model. *Sci Rep*. 2019;9(1):13592.
- Wang X, Zhang XG, Zhou TT, Li N, Jang CY, Xiao ZC, et al. Elevated neuronal excitability due to modulation of the voltage-gated sodium channel Nav1.6 by A β 1–42. *Front Neurosci*. 2016;10:94.
- Shah NH, Aizenman E. Voltage-gated potassium channels at the crossroads of neuronal function, ischemic tolerance, and neurodegeneration. *Transl Stroke Res*. 2014;5(1):38–58.
- Yin H, Wang H, Zhang H, Gao N, Zhang T, Yang Z. Resveratrol attenuates A β -induced early hippocampal neuron excitability impairment via recovery of function of potassium channels. *Neurotox Res*. 2017;32(3):311–24.
- Ping Y, Hahn ET, Waro G, Song Q, Vo-Ba DA, Licursi A, et al. Linking a β 42-induced hyperexcitability to neurodegeneration, learning and motor deficits, and a shorter lifespan in an Alzheimer's model. *PLoS Genet*. 2015;11(3):1005025.
- Feng G, Pang J, Yi X, Song Q, Zhang J, Li C, et al. Down-regulation of K(V)4 channel in drosophila mushroom body neurons contributes to A β 42-induced courtship memory deficits. *Neuroscience*. 2018;370:236–45.
- Beaudoin GM 3rd, Lee SH, Singh D, Yuan Y, Ng YG, Reichardt LF, et al. Culturing pyramidal neurons from the early postnatal mouse hippocampus and cortex. *Nat Protoc*. 2012;7(9):1741–54.
- Wang YX, Xia ZH, Jiang X, Li LX, An D, Wang HG, et al. Genistein inhibits A β 25–35-induced neuronal death with changes in the electrophysiological properties of voltage-gated sodium and potassium channels. *Cell Mol Neurobiol*. 2019;39(6):809–22.
- Tamano H, Nishio R, Shakushi Y, Sasaki M, Koike Y, Osawa M, et al. In vitro and in vivo physiology of low nanomolar concentrations of Zn(2+) in artificial cerebrospinal fluid. *Sci Rep*. 2017;7:42897.
- Frederickson CJ, Giblin LJ, Krezel A, McAdoo DJ, Mueller RN, Zeng Y, et al. Concentrations of extracellular free zinc (pZn) in the central nervous system during simple anesthetization, ischemia and reperfusion. *Exp Neurol*. 2006;198(2):285–93.
- Sensi SL, Paoletti P, Koh JY, Aizenman E, Bush AI, Hershfinkel M. The neurophysiology and pathology of brain zinc. *J Neurosci*. 2011;31(45):16076–85.
- Paoletti P, Vergnano AM, Barbour B, Casado M. Zinc at glutamatergic synapses. *Neuroscience*. 2009;158(1):126–36.
- Colvin RA, Bush AI, Volitakis I, Fontaine CP, Thomas D, Kikuchi K, et al. Insights into Zn²⁺ homeostasis in neurons from experimental and modeling studies. *Am J Physiol Cell Physiol*. 2008;294(3):C726–42.
- Tougu V, Karafin A, Palumaa P. Binding of zinc(II) and copper(II) to the full-length Alzheimer's amyloid-beta peptide. *J Neurochem*. 2008;104(5):1249–59.
- Takeda A, Koike Y, Osawa M, Tamano H. Characteristic of extracellular Zn(2+) influx in the middle-aged dentate gyrus and its involvement in attenuation of LTP. *Mol Neurobiol*. 2018;55(3):2185–95.
- Beyer N, Coulson DT, Heggarty S, Ravid R, Irvine GB, Hellems J, et al. ZnT3 mRNA levels are reduced in Alzheimer's disease post-mortem brain. *Mol Neurodegener*. 2009;4:53.
- Adlard PA, Parmcutt JM, Finkelstein DI, Bush AI. Cognitive loss in zinc transporter-3 knock-out mice: a phenocopy for the synaptic and memory deficits of Alzheimer's disease? *J Neurosci*. 2010;30(5):1631–6.
- Koh JY, Lee SJ. Metallothionein-3 as a multifunctional player in the control of cellular processes and diseases. *Mol Brain*. 2020;13(1):116.

47. Wang R, Reddy PH. Role of glutamate and NMDA receptors in Alzheimer's disease. *J Alzheimers Dis*. 2017;57(4):1041–8.
48. Ji SG, Medvedeva YV, Wang HL, Yin HZ, Weiss JH. Mitochondrial Zn(2+) accumulation: a potential trigger of hippocampal ischemic injury. *Neuroscientist*. 2019;25(2):126–38.
49. Forostyak O, Forostyak S, Kortus S, Sykova E, Verkhatsky A, Dayanithi G. Physiology of Ca(2+) signalling in stem cells of different origins and differentiation stages. *Cell Calcium*. 2016;59(2–3):57–66.
50. Colbourne F, Grooms SY, Zukin RS, Buchan AM, Bennett MV. Hypothermia rescues hippocampal CA1 neurons and attenuates down-regulation of the AMPA receptor GluR2 subunit after forebrain ischemia. *Proc Natl Acad Sci U S A*. 2003;100(5):2906–10.
51. Liu S, Lau L, Wei J, Zhu D, Zou S, Sun HS, et al. Expression of Ca(2+)-permeable AMPA receptor channels primes cell death in transient forebrain ischemia. *Neuron*. 2004;43(1):43–55.
52. Stork CJ, Li YV. Rising zinc: a significant cause of ischemic neuronal death in the CA1 region of rat hippocampus. *J Cereb Blood Flow Metab*. 2009;29(8):1399–408.
53. Yang JS, Jeon S, Yoon KD, Yoon SH. Cyanidin-3-glucoside inhibits amyloid β (25–35)-induced neuronal cell death in cultured rat hippocampal neurons. *Korean J Physiol Pharmacol*. 2018;22(6):689–96.
54. Xia Q, Wang H, Yin H, Yang Z. Excessive corticosterone induces excitotoxicity of hippocampal neurons and sensitivity of potassium channels via insulin-signaling pathway. *Metab Brain Dis*. 2019;34(1):119–28.
55. Villa C, Suphesiz H, Combi R, Akyuz E. Potassium channels in the neuronal homeostasis and neurodegenerative pathways underlying Alzheimer's disease: an update. *Mech Ageing Dev*. 2020;185:111197.
56. Mitterdorfer J, Bean BP. Potassium currents during the action potential of hippocampal CA3 neurons. *J Neurosci*. 2002;22(23):10106–15.
57. Shan D, Xie Y, Ren G, Yang Z. Inhibitory effect of tungsten carbide nanoparticles on voltage-gated potassium currents of hippocampal CA1 neurons. *Toxicol Lett*. 2012;209(2):129–35.
58. Mayer ML, Vyklicky L Jr. The action of zinc on synaptic transmission and neuronal excitability in cultures of mouse hippocampus. *J Physiol*. 1989;415:351–65.
59. Chung J, Chang S, Kim Y, Shin H. Zinc increases the excitability of dopaminergic neurons in rat substantia nigra. *Neurosci Lett*. 2000;286(3):183–6.
60. Noh J, Chang SY, Wang SY, Chung JM. Dual function of Zn²⁺ on the intrinsic excitability of dopaminergic neurons in rat substantia nigra. *Neuroscience*. 2011;175:85–92.
61. Degirmenci S, Olgar Y, Durak A, Tuncay E, Turan B. Cytosolic increased labile Zn(2+) contributes to arrhythmogenic action potentials in left ventricular cardiomyocytes through protein thiol oxidation and cellular ATP depletion. *J Trace Elem Med Biol*. 2018;48:202–12.
62. Teisseyre A, Mercik K, Mozrzymas JW. The modulatory effect of zinc ions on voltage-gated potassium currents in cultured rat hippocampal neurons is not related to Kv1.3 channels. *J Physiol Pharmacol*. 2007;58(4):699–715.
63. Zhang F, Ma XL, Wang YX, He CC, Tian K, Wang HG, et al. TPEN, a specific Zn(2+) chelator, inhibits sodium dithionite and glucose deprivation (SDGD)-induced neuronal death by modulating apoptosis, glutamate signaling, and voltage-gated K(+) and Na(+) channels. *Cell Mol Neurobiol*. 2017;37(2):235–50.
64. Li Y, Andereggen L, Yuki K, Omura K, Yin Y, Gilbert HY, et al. Mobile zinc increases rapidly in the retina after optic nerve injury and regulates ganglion cell survival and optic nerve regeneration. *Proc Natl Acad Sci U S A*. 2017;114(2):E209–e218.
65. Trakhtenberg EF, Li Y, Feng Q, Tso J, Rosenberg PA, Goldberg JL, et al. Zinc chelation and Klf9 knockdown cooperatively promote axon regeneration after optic nerve injury. *Exp Neurol*. 2018;300:22–9.
66. Yu Z, Yu Z, Chen Z, Yang L, Ma M, Lu S, et al. Zinc chelator TPEN induces pancreatic cancer cell death through causing oxidative stress and inhibiting cell autophagy. *J Cell Physiol*. 2019;234(11):20648–61.

Publisher's Note

Springer Nature remains neutral with regard to jurisdictional claims in published maps and institutional affiliations.

Ready to submit your research? Choose BMC and benefit from:

- fast, convenient online submission
- thorough peer review by experienced researchers in your field
- rapid publication on acceptance
- support for research data, including large and complex data types
- gold Open Access which fosters wider collaboration and increased citations
- maximum visibility for your research: over 100M website views per year

At BMC, research is always in progress.

Learn more biomedcentral.com/submissions

